Post-Stack Stochastic Inversion - Bualuang Field, Gulf of Thailand

Rudranath Mukherjee(CGG–Mumbai), Rakesh Bharat Doshi (CGG-Kuala Lumpur), Rajat Rathore (CGG–Singapore)*

Hans Girling, Jaume Vendrell (Salamander Energy - an Ophir Group Company, Bangkok, Thailand)

rudranath.mukherjee@cgg.com

Keywords

Stochastic Inversion, Post Stack, P-Impedance, Effective Porosity

Summary

The Bualuang Field is located in western Gulf of Thailand (concession block number B8/38). Salamander Energy, an Ophir Group company assumed operatorship of the field on March 2008 and the field has been on-stream since August 2008.

This field has been penetrated by around 60 wells. A static model built purely from well constraints was available in this study. However, this model lacked lateral heterogeneity of the reservoir. Hence, a high resolution characterization of this field was performed to integrate the various available data at a fine scale. Due to a limitation in the seismic data, only post stack information is available. As such, a post stack geostatistical inversion was performed to generate multiple equi-probable volumes of P-Impedance and Effective Porosity which conforms to all available input data. The multiple realizations were then used for uncertainty quantification of reservoir properties.

Introduction

The Bualuang oil field consists of two distinct but related structures: the Main Fault Block and the East Terrace (Figure 1). Within these structures oil occurs in a number of independent reservoirs (Figure 2) which are all formed by Miocene sandstones deposited in fluvial settings. By far the most important reservoir, which contains the bulk of the field's oil in place, is known as the T4.1 sand. Recent production wells in the Main Fault block have targeted the older T2 Sand, and these wells, which are now on production, have confirmed the commercial viability of this reservoir. In the Main Fault block oil has also been encountered in the younger T5.2 Sand, although this reservoir has yet to be fully brought on production.

The East Terrace was drilled by two exploration wells which confirmed tens of meters of stacked pay in both the northern and central structures. Since then, various development wells, in different reservoir levels have been completed as producing wells on the East Terrace.

The various reservoirs that comprise the Bualuang oil field have distinctly different parameters even though they were all deposited in fluvial settings. The T4.1 sand was deposited in a high energy braided river system. As a result the gross morphology of the reservoir comprises of massive amalgamated sheet-like sands with little of the lateral or vertical variability normally associated with distinct channel bodies. Reservoir parameters are uniformly excellent with porosities exceeding 30% and permeability often in excess of one Darcy. Although in places the reservoir degrades towards the top, reservoir continuity is maintained field-wide. As bottom water is present across the field the excellent reservoir quality and low GOR oil means that water break through and water coning are potential production issues, particularly during the late stages of individual well lives.

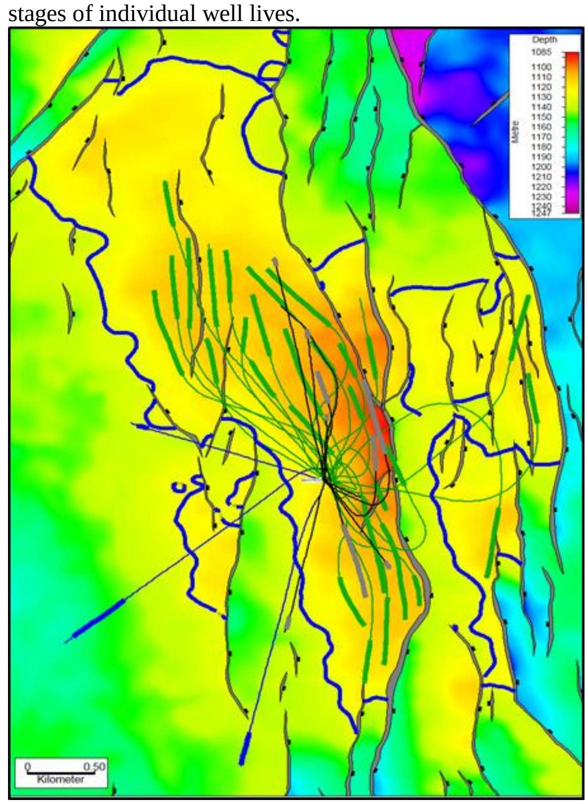

Figure 1: Bualuang Field structure map on top T4.1 (main Reservoir).

The other productive reservoirs (T5, T3, and T2) are developed in meandering fluvial systems with discreet channel geometry and better developed over-bank mudstone sequences. In these sandstones the reservoir parameters are relatively poorer (although nonetheless still good) with lower net to gross, porosity (20 – 25%) and permeability (hundreds of millidarcies). Bottom water is not an issue in these reservoirs and results from the T2 producers suggest aquifer support from edge water.

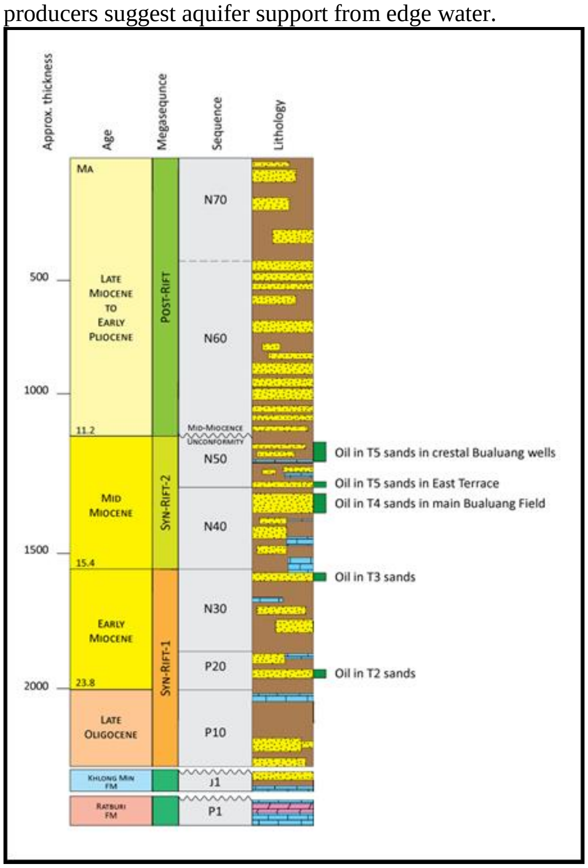

Figure 2: Offshore Gulf of Thailand stratigraphy highlighting productive reservoirs in the Bualuang Field.

Method

To estimate the reservoir potential accurately, an integrated study is required which involves a variety of input information e.g. wells, seismic, sequence stratigraphy and etc. Sams *et. al.* and Rakesh *et. al.* discussed two different workflows to integrate various information to perform a high resolution reservoir characterization. For this study, a post stack Markov Chain Monte Carlo Geostatistical Inversion algorithm was used to integrate all the measured (well, seismic) and modelled data (interpretation, sequence stratigraphy, probability density functions, Variograms) at a fine scale. The benefit of this method is a joint inversion of the impedance and lithology. The workflow adapted is summarized in Figure 3.

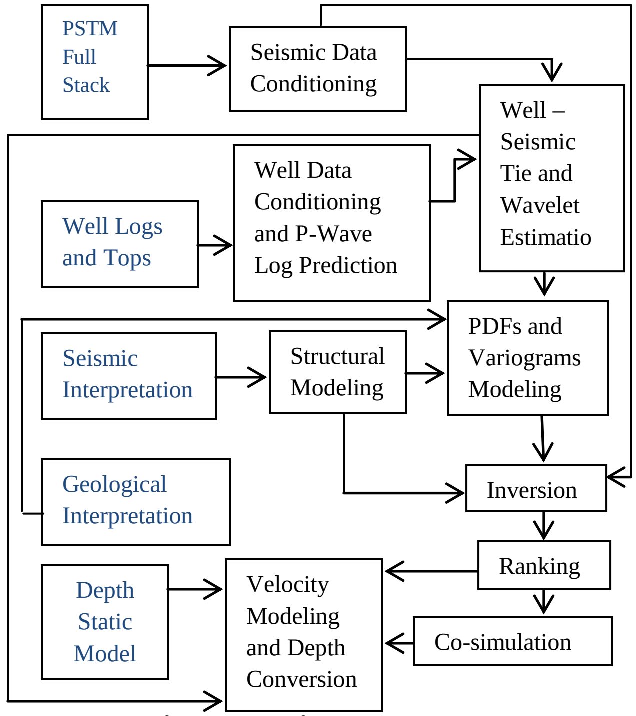

Figure 3: Workflow adopted for this study. The inputs are highlighted in blue.

Seismic Data Conditioning

During the acquisition of 3D seismic data, the presence of surface facilities left a 2.5km^2 gap in the acquired seismic cube. Moreover, a limited cable length presented this issue in all offsets. In order to overcome this problem, 2D lines predating the installation of the surface facilities were interpolated into a pseudo-3D and used to infill the gap in the seismic data. However, this process was carried out in the post-stack domain and resulted in slight differences in amplitude gain across the two datasets. Amplitude compensation was applied to the seismic data to overcome the observed amplitude differences (as shown in Figure 4),

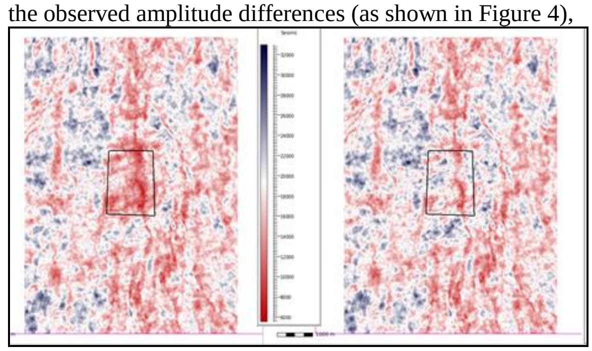

Figure 4: RMS amplitude map of the reservoir zone. Map showing dim amplitude before scaling (left), which was subsequently corrected after scaling (right).

prior to utilizing the seismic cube for reservoir characterization studies. A simple amplitude compensation workflow utilizing a spatially filtered scalar map derived from the RMS seismic amplitude was applied to the seismic data. This resulted in a better continuity of seismic data

Well Data Conditioning

Log data for a total of 24 vertical and semi-vertical wells were available for this study. During the petrophysical evaluation and QC stage, this log data was conditioned for washout effects and spurious values. Among the 24 wells used in the inversion either directly (constrained wells) or indirectly (blind wells for QC), only 9 wells had P-wave logs available. The P-wave log for the remaining wells was synthesized using a multi-linear regression approach. All other available logs such as Density, Gamma Ray, Neutron and Deep Resistivity were used as inputs to the multi linear regression process. Also, different regressions were applied for Oil Sand, Brine Sand and Shale. Figure 5 show that the synthesized curve (blue curve in track 4) clearly has a high correlation with the measured curve (pink).

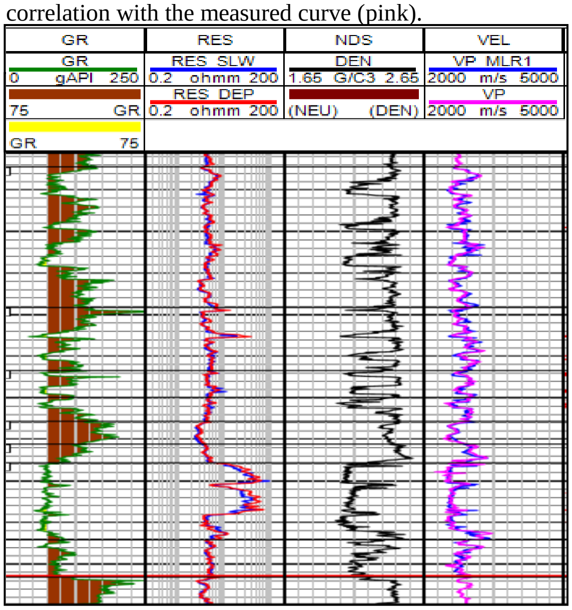

Figure 5: P-wave synthesis via multi-linear regression. The well sonic is displayed in blue in track 4 while the synthesized p-sonic is displayed in pink.

Structural Modelling

To incorporate the sequence stratigraphy and difference in morphology of the fluvial sands in the different reservoir levels, a structural model was prepared with the available TWT seismic horizons and major faults. As it was described earlier, a thick and laterally extensive channel belt dominates the deeper part of the reservoir zone while the channel bodies in the shallower part of the reservoir are of a different geometry. The orientation of the channel bodies is also different in the different reservoir intervals. Hence, in order to account for the non-stationarity, the entire reservoir zone was divided into three different intervals. Care was taken to avoid any leakage in the structural framework. The final structural model is a solid model with three reservoir layers, intersected and displaced by faults, as shown in Figure 6.

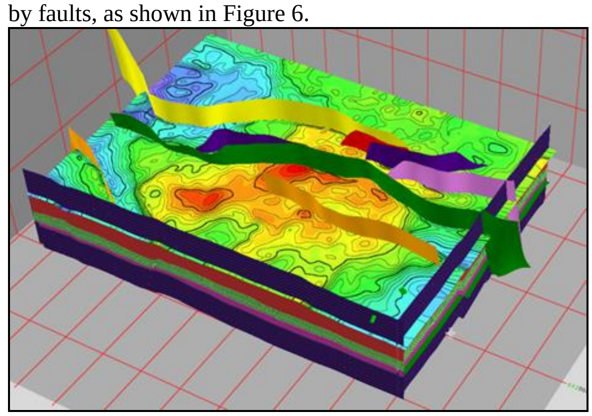

Figure 6: Structural Model used for inversion.

Stochastic Inversion

During the seismic to well tie stage several wells were dropped from the inversion process due to their poor correlation with the seismic data. As a result, only 14 wells were finally incorporated in the inversion study.

Unlike deterministic inversion, this algorithm does not need a physical *a priori* model to be built. The *a priori* model is simulated based on the input data and the user defined uncertainty bounds. This simulation process begins with simulation of the facies properties and updates it based on the seismic to synthetic tie.

For this study, the simulation was based on sand and shale facies. Based on the simulated facies, a random draw of P-Impedance coupled with seismic to synthetic tie either accepted or rejected the particular simulation.

Multiple simulations of sand and shale facies provided means for uncertainty quantification. A total of 21 realizations of sand/shale facies were simulated which then also resulted in 21 realizations of P-Impedance (and finally the same amount of PHIE volumes).

During the simulation process, it was also imperative that the simulated models adhere to the given spatio-temporal statistics. The vertical variograms from well logs were measured to be 6 to 16 ms while the lateral variograms from seismic amplitudes were estimated to be varying within 475 m to 600 m for the different intervals.

Also, the variability in the quality of the seismic is taken into consideration in the simulation process. Either a constant or variable S/N ratio can be used to define the quality of the input seismic data. After numerous tests a map of S/N was chosen as an input to take into account the spatially varying confidence in the seismic data.

After completing the inversion, we then performed a co-simulation of PHIE with P-Impedance. For each realization of P-Impedance, we simulated a PHIE volume from the PDF function which was defined by the well data. Figure 7 shows an example of the PDF data in one of the intervals.

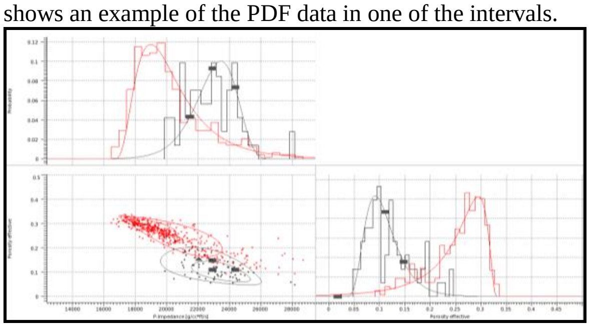

Figure 7: Co-simulation of PHIE and P-Impedance for sand (red) and shale (black) facies.

Another objective of this study was to convert the P-Impedance and PHIE volumes into depth so that they could be used as a direct input to the static model (in depth domain). Although time and depth horizons were made available for this study, minor corrections to the depth-time relationship was required in view of the update performed during the seismic to well tie process. To achieve this, a velocity model was built from the final depth to time relationship and was populated into the structural model which was locally flexed to account for the update in the time to depth relationship. Finally, a velocity calibration process was undertaken by constraining the depths based on the given depth interpretations.

Geostatistical Inversion Results QC

Various quality control procedures were undertaken to ensure optimal quality inversion results were obtained. Figure 8 displays one of the main QC- the goodness of fit of the synthetic data to the given seismic data. A high correlation value is observed almost everywhere with only a slightly degraded match observed at the faults. Figure 9 displays the same QC in a section view. Once again, the top figure shows that the inversion is able to fully explain the given seismic data.

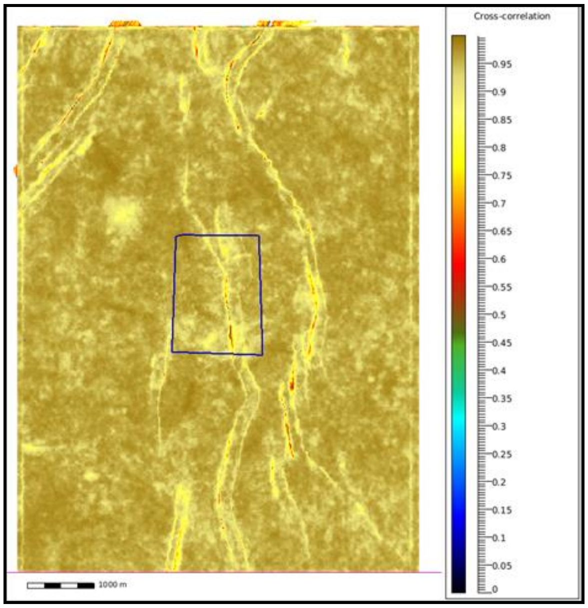

Figure 8: Synthetic-Seismic correlation. The lower values are at the fault locations.

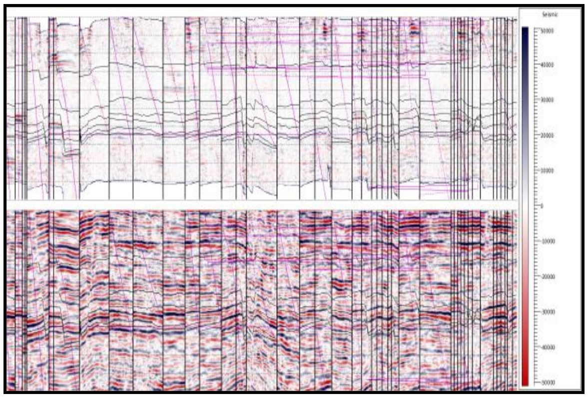

Figure 9: Inverted Residual (above) and input seismic (below). The inversion window between the horizons does not show any residuals.

The ultimate QC of any inversion results is the goodness of fit of the elastic (or petrophysical) properties at blind well locations. Figure 10 compares the well P-Impedance against the mean P-Impedance +/- 1 standard deviation envelope along the well trajectory. This QC clearly shows that despite these wells being blind wells (wells not used in any process of the inversion), the inversion has been able to predict the well data with reasonable accuracy. In Figure 11, the QC of the simulated PHIE (from one realization) against the well PHIE at blind well locations is shown. Once again, the inversion is able to predict the well property with reasonable accuracy.

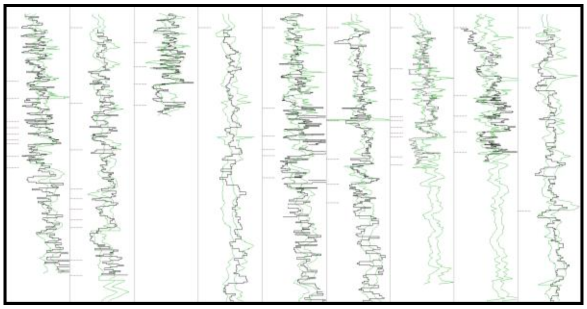

Figure 10: Blind well QC of P-Impedance. The corridor of the green curves displays the mean +/- 1 standard deviation of the P-Impedance along the well trajectory while the black trace is the well log.

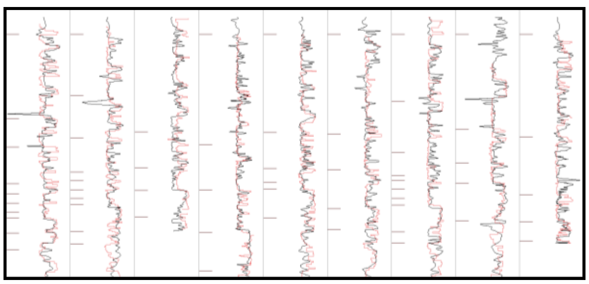

Figure 11: Blind well QC of PHIE. The black curve is that of the well data while the red trace is the simulated PHIE along the well trajectory.

Co-simulated PHIE volume

With good confidence in the inversion results, we were then able to update the static model with the simulated PHIE volume. Figure 12 compares the PHIE volume from the previously built static model against the simulated PHIE from the inversion results. At the time of writing this paper, we were postulating on which is the best method to include the simulated PHIE in the static model. This will perhaps be the subject of another paper.

Interpretation of Results

The entire reservoir zone is comprised of sand bodies of different thickness and shape. These channel sands were interpreted in the existing seismic volume. So, on completion of the Inversion & Co-simulation, another QC is performed to check if the result is satisfactory to match/ enhance these geological interpretations. To do so, stratal-slices between each reservoir layer are created from the Litho-facies, P-Impedance & Effective Porosity volumes The channel bodies picked up from these slices have a very good match with the existing geological interpretation. One example in the top reservoir layer is shown in Figure 13.

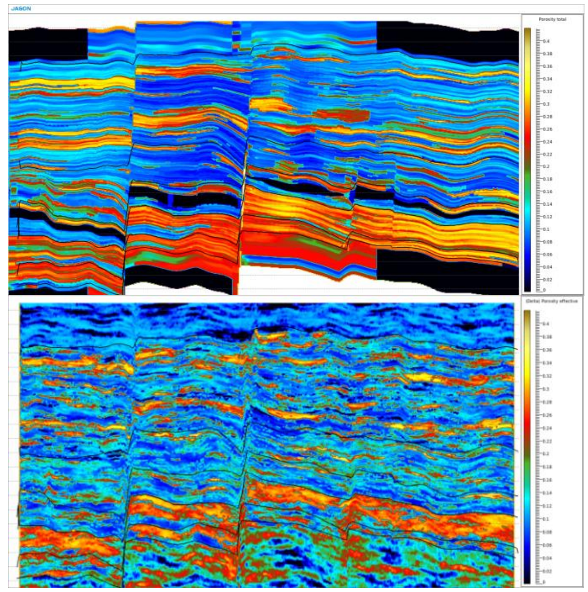

Figure 12: Comparison between the previous static model (top) and one of the geostatistically simulated PHIE volume (below).

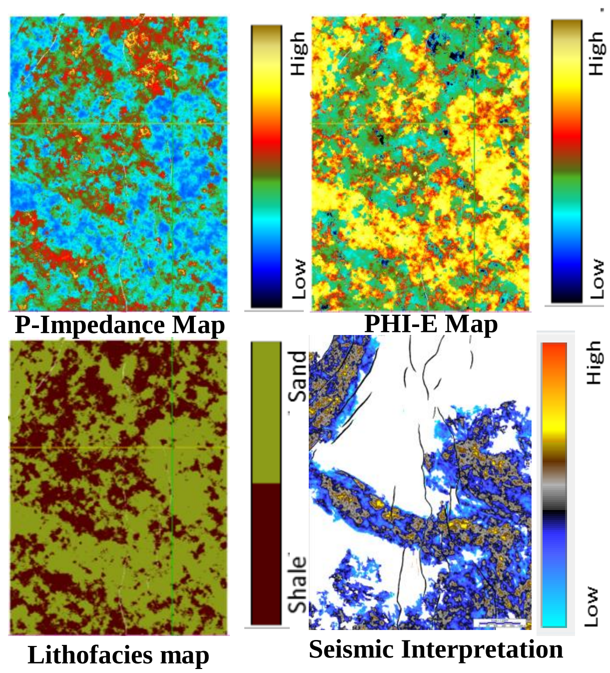

Figure 13. The channel sand as interpreted from seismic amplitude map is also seen in the P-Impedance & lithology map. Also, the result is more pronounced in the Effective Porosity map.

Conclusions

The Stochastic inversion workflow adopted here is successful in performing a high resolution reservoir characterization of Bualuang Field. This is supported by numerous blind well QC. Despite limitations in the seismic data, multiple PHIE models with good confidence, as ascertained from various QC, were available for update of the static model.

References

M. S. Sams, D. Atkins, N. Said, E. Pareito, P. van Rief, 1999, Stochastic Inversion for High Resolution Reservoir Characterization in the Central Sumatra Basin, SPE 57260

Rakesh Doshi, Loic Michel, Rachim Winata Abdul, Rangga Brahmantio, Gilles Vallon, 2013, Stochastic Seismic Lithofacies Classification Over Sisi Nubi Field, 37th IPA Proceeding

Acknowledgements

We would like to thank Salamander Energy - an Ophir Group Company and CGG for permissions to publish this work. The authors would like to thank their colleagues especially Jiun Yap, Jimmy Ting and Ranjit Shaw for constructive discussions and recommendations towards the betterment of the outcome of this study.